High-resolution study of Gamow-Teller transitions from the $T_z = 1$ nucleus ^{46}Ti to the $T_z = 0$ nucleus ^{46}V

T. Adachi,[1,*] Y. Fujita,[1,†] P. von Brentano,[2,‡] A. F. Lisetskiy,[3] G. P. A. Berg,[4,§] C. Fransen,[2] D. De Frenne,[5] H. Fujita,[1,‖] K. Fujita,[6] K. Hatanaka,[6] M. Honma,[7] E. Jacobs,[5] J. Kamiya,[6,¶] K. Kawase,[6] T. Mizusaki,[8] K. Nakanishi,[6] A. Negret,[5,**] T. Otsuka,[9] N. Pietralla,[2,††] L. Popescu,[5,**] Y. Sakemi,[6] Y. Shimbara,[1,‡‡] Y. Shimizu,[6] Y. Tameshige,[6] A. Tamii,[6] M. Uchida,[6,§§] T. Wakasa,[6,‖‖] M. Yosoi,[6] and K. O. Zell[2]

[1]*Department of Physics, Osaka University, Toyonaka, Osaka 560-0043, Japan*
[2]*Institut für Kernphysik, Universität zu Köln, D-50937 Köln, Germany*
[3]*NSCL, Michigan State University, East Lansing, Michigan 48824, USA*
[4]*Kernfysisch Versneller Instituut, Zernikelaan 25, 9747 AA Groningen, The Netherlands*
[5]*Vakgroep Subatomaire en Stralingsfysica, Universiteit Gent, B-9000 Gent, Belgium*
[6]*Research Center for Nuclear Physics, Osaka University, Ibaraki, Osaka 567-0047, Japan*
[7]*Center for Mathematical Science, University of Aizu, Aizu-Wakamatsu, Fukushima 965-8580, Japan*
[8]*Institute of Natural Science, Senshu University, Tama, Kawasaki, Kanagawa 214-8580, Japan*
[9]*Department of Physics, University of Tokyo, Hongo, Bunkyo, Tokyo 113-0033, Japan*

(Received 11 October 2005; published 15 February 2006)

The Gamow-Teller (GT) transition strengths in *fp*-shell nuclei are important parameters in presupernova models. A high-energy-resolution (^{3}He, t) experiment was performed on the $T_z = 1$ nucleus ^{46}Ti at 0° and at an intermediate incident energy of 140 MeV/nucleon for the study of precise GT transition strengths to the final $T_z = 0$ nucleus ^{46}V. With an energy resolution of 33 keV, individual GT transitions were observed and GT strengths were derived for them up to the excitation energy of 4.5 MeV. The GT strengths were compared with shell-model calculations using various effective interactions. In this low-lying region, most GT states have isospin $T = 0$. A few GT states with isospin $T = 1$ were identified from the existence of the corresponding (analog) $M1$ states in ^{46}Ti. By comparing the GT strength with the corresponding (analogous) $M1$ transition strength studied in ^{46}Ti(e, e') or (γ, γ') measurements, a large constructive interference of orbital and spin terms was suggested for one of these $M1$ transitions.

DOI: 10.1103/PhysRevC.73.024311 PACS number(s): 25.55.Kr, 21.10.Hw, 21.60.Cs, 27.40.+z

I. INTRODUCTION

Gamow-Teller (GT) transitions play important roles in the universe. At the end of the evolution of a massive star, if the iron core in the center exceeds the Chandrasekhar mass limit, the electron degeneracy pressure can no longer support the core that produces no energy by the nuclear fusion, and the star starts to collapse. This is the beginning of a type II supernova [1]. In this early stage of the collapse, electron capture and β decay of *fp*-shell nuclei become important nuclear processes. Under supernova conditions electron capture and β decay are dominated by GT (and also by Fermi) transitions. The weak-interaction rates used in presupernova models were systematically but phenomenologically estimated by Fuller, Fowler, and Newman [2] for nuclei with masses $A < 60$ despite the difficulty that no experimental data were available in the beginning of the 1980s.

The most direct information on the GT transition strength B(GT) can be obtained from β-decay studies, but the accessible excitation energies (E_x) are limited by the decay Q values. Charge-exchange (CE) reactions, such as (p, n) or (^{3}He, t) reactions, can access GT transitions at higher energies without this Q-value limitation. In particular, measurements at angles around 0° and at intermediate incident energies above 100 MeV/nucleon were shown to be good probes of GT transition strengths owing to the approximate proportionality between the CE cross sections at 0° and the B(GT) values [3].

Experimental measurements of GT strength distributions gradually became available in the 1980s by using (p, n) and (n, p) reactions at intermediate beam energies [4]. With typical energy resolutions of 300 keV and 1 MeV in the (p, n) and (n, p) measurements, respectively, these studies revealed the overall distributions of the GT strengths for *fp*-shell nuclei.

*Electronic address: adachi@rcnp.osaka-u.ac.jp
†Electronic address: fujita@rcnp.osaka-u.ac.jp
‡Electronic address: brentano@ikp.uni-koeln.de
§Present address: Department of Physics, University of Notre Dame, Notre Dame, IN 46556, USA.
‖Present address: iThemba LABS, P.O. Box 722, Somerset West 7129, South Africa.
¶Present address: Japan Atomic Energy Research Institute, Tokai, Ibaraki 319-1195, Japan.
**Permanent address: NIPNE, Str. Atomistilor no. 407, P. O. Box MG-6, Bucharest, Romania.
††Present address: Nuclear Structure Lab., Department of Physics and Astronomy, State University of New York, Stony Brook, NY 11794-3800.
‡‡Present address: NSCL, Michigan State University, East Lansing, MI 48824, USA.
§§Present address: Department of Physics, Tokyo Institute of Technology, Oh-okayama, Meguro, Tokyo 152-8550, Japan.
‖‖Present address: Department of Physics, Kyushu University, Higashi, Fukuoka 812-8581, Japan.

 ©2006 The American Physical Society

Recently, state-of-the-art techniques developed in the shell model made the calculation of GT strengths in the *fp*-shell feasible [5–7]. The overall GT distributions could be reproduced well and encouraged by these successes, calculations were extended to the region of unstable nuclei where the above reactions are not feasible at present [8,9]. It is, however, important to note that the GT strength is fragmented over many discrete states in the *fp*-shell nuclei, and the details of the strength distributions are important in presupernova models. Therefore, knowledge of the experimental GT distributions should be elaborated and the theoretical calculations should be made to reproduce them.

With the development of precise beam matching techniques [10], a very good energy resolution ΔE of $<$50 keV was realized in recent (^{3}He, t) measurements at 0° and at intermediate incident energies [11]. The validity of the approximate proportionality between the cross sections at 0° and the B(GT) values has been demonstrated in the (^{3}He, t) measurements for states with an "$L = 0$" nature and for values of $B(\mathrm{GT}) \geqslant 0.04$ [12,13]. Therefore, states unresolved in earlier CE measurements could be clearly resolved, and more stringent comparisons with theoretical calculations can be performed. A typical example was a comparison of experimental and shell-model B(GT) distributions at the middle of the *fp* shell. The detailed B(GT) distribution studied in the ^{58}Ni(^{3}He, t)^{58}Cu [14] was a challenge for shell-model calculations using the modern shell-model interactions FPD6 [15], KB3G [14], and GXPF1 [6].

As an extension of these studies, we started to examine GT transitions in nuclei in the beginning of the *fp* shell. In this article, the $T_z = 1$ nucleus ^{46}Ti was selected as target, and GT transitions to the odd-odd $T_z = 0$ nucleus ^{46}V were examined. The obtained GT strength distribution is compared with the results of the modern shell-model calculations.

II. EXPERIMENT

At intermediate energies ($\geqslant$100 MeV/nucleon) and at forward angles including 0°, GT states become prominent in (^{3}He, t) reactions, because of their $L = 0$ nature and the dominance of the $\sigma\tau$ part of the effective nuclear interaction [16]. The ^{46}Ti(^{3}He, t)^{46}V measurement was performed at the high-resolution facility of RCNP, Osaka, consisting of the "WS course" [17] and the Grand Raiden spectrometer [18] placed at 0° using a 140 MeV/nucleon ^{3}He beam from the $K = 400$ Ring Cyclotron [19]. The ^{3}He beam was stopped by a Faraday cup inside the first dipole magnet.

The large difference of atomic energy losses of ^{3}He and tritons in a target can cause a large energy spread of the outgoing tritons if the target is not thin enough. Thus, a rather thin self-supporting enriched metallic foil of ^{46}Ti with an isotopic enrichment of 86.1(1)% and an areal density of 0.92(5) mg/cm^2 was used. It also contained 10.6(1)% of ^{48}Ti, 1.6(1)% of ^{47}Ti, 1.0(1)% of ^{50}Ti, and 0.8(1)% of ^{49}Ti. The outgoing tritons within the full acceptance of the spectrometer [$\approx \pm 20$ mr and $\approx \pm 40$ mr in horizontal (x) and vertical (y) directions, respectively] were momentum analyzed and detected at the focal plane with a multiwire drift-chamber system allowing track reconstruction [20]. The acceptance of the spectrometer was subdivided in scattering-angle regions in the analysis using the track information.

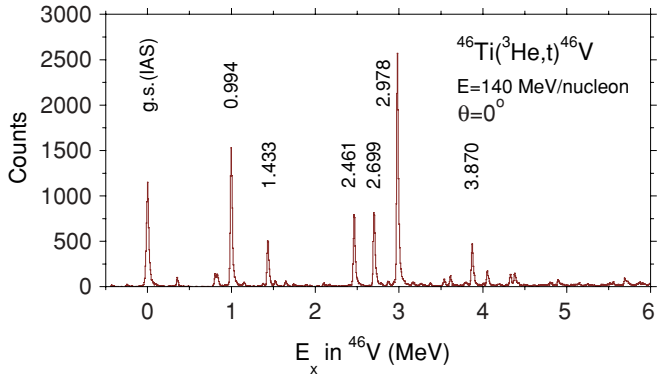

FIG. 1. (Color online) The 0° ^{46}Ti(^{3}He, t)^{46}V spectrum. The events with scattering angles $\Theta \leqslant 0.5°$ are included. The energy resolution of 33 keV made it possible to observe discrete states in the excitation energy region up to 6 MeV. Major $L = 0$ states of ^{46}V are indicated by their excitation energies in megaelectron volts.

An energy resolution of 33 keV [full width at half maximum (FWHM)], which is better by about a factor of 5 than the energy spread of the beam, was realized by applying *dispersion matching* and *focus matching* techniques [10]. For fast and efficient beam tuning, the "faint beam method" [21,22] was applied. Owing to the high energy resolution, many well-separated states were observed. The "0° spectrum" of the ^{46}Ti target with scattering angles $\Theta \leqslant 0.5°$ is shown in Fig. 1.

To identify states originating from ^{48}Ti in the ^{46}Ti(^{3}He, t)^{46}V spectrum, a spectrum from an enriched ^{48}Ti foil (enrichment 99.1%) was measured under the same condition as for the ^{46}Ti target. By a comparison of both spectra, it was found that several relatively weak peaks originated from ^{48}Ti. In addition, a ^{47}Ti(^{3}He, t)^{47}V spectrum from an enriched ^{47}Ti foil was measured. By comparing the ^{46}V and ^{47}V spectra, several very weak peaks originating from ^{47}Ti were identified in the ^{46}V spectrum. The ^{46}V states that are clearly observed in the 0° spectrum are indicated by their excitation energies in Fig. 1 and listed in Table I.

To accurately determine the scattering angle Θ near 0°, scattering angles in both x direction (θ) and y direction (ϕ) should be measured equally well, where Θ is defined by $\sqrt{\theta^2 + \phi^2}$. Good θ resolution was achieved by using the *angular dispersion matching* technique [10], whereas good ϕ resolution was achieved by applying the "over-focus mode" of the spectrometer [24]. The angle calibration was performed by using a multihole aperture. The "0° spectrum" in Fig. 1 shows events for the scattering angles $\Theta \leqslant 0.5°$. As shown below, all prominent states are of $L = 0$ nature.

Very little was known for the $L = 0$ states in ^{46}V. The ground state (g.s.) of ^{46}V is the $J^\pi = 0^+$ isobaric analog state (IAS) of the target nucleus ^{46}Ti [23]. Clear assignment of $J^\pi = 1^+$ and an accurate E_x value with an uncertainties of less than 1 keV was given only for the 0.994 MeV state [23,25] (see Table I). Therefore, E_x values of other excited states were determined in comparison with a reference spectrum measured

TABLE I. States observed in the ^{46}Ti(^{3}He, t)^{46}V reaction for excitation energies below 4.5 MeV. For the $L = 0$ states, except for the $J^\pi = 0^+$ g.s. (IAS), GT transition strengths B(GT) are given. For details of the uncertainties of B(GT) values, see text.

Evaluated values[a]		(^{3}He, t)[b]		
E_x (MeV)	J^π	E_x (MeV)	L	B(GT)
0.0	0^+	0.0	0	
0.801(1)	3^+	0.803	$\geqslant 1$	
0.9936(3)	1^+	0.994	0	0.365(44)
1.3761(1)	3^+	1.375	$\geqslant 1$	
1.4318(5)	(1, 2)	1.433	0	0.124(15)
2.449(15)	(1^+, 2^+)	2.461	0	0.195(24)
2.686(15)		2.699	0	0.206(25)
2.8676(12)		2.867	$\geqslant 1$	
2.977(15)		2.978	0	0.604(73)
		3.535	0	0.019(3)
3.615(15)		3.610	0	0.025(4)
3.871(15)		3.870	0	0.117(14)
		4.051	0	0.043(6)
		4.325	0	0.034(5)
		4.378	0	0.037(5)

[a]From Ref. [23].
[b]Present work.

under the same condition as for the ^{46}Ti and ^{48}Ti targets. Accurate E_x values with uncertainties of less than 1 keV are known for the 1^+ states of ^{26}Al up to 7.9 MeV and for a few states in ^{24}Al [26]. In addition, E_x values of several low J states are known in ^{16}F [27]. Those states that were observed in the spectrum from a thin target foil of $^{nat}MgCO_3$ supported by polyvinylalcohol (PVA) [28] made it possible to consistently determine the E_x values of the states in ^{46}V with the help of kinematic calculations. All E_x values of these states in ^{46}V shown in column 3 of Table I could be determined by interpolation. We estimate uncertainties of less than 4 keV for all states up to 4.5 MeV.

Owing to the *angular dispersion matching* and also to the overfocus mode of the spectrometer setting, it is estimated that an angle resolution better than 5 mr was achieved [24]. To identify the $L = 0$ nature of states, relative intensities of the peaks were examined for the spectra with the angle cuts $\Theta = 0^\circ - 0.5^\circ$, $0.5^\circ - 1.0^\circ$, $1.0^\circ - 1.5^\circ$, and $1.5^\circ - 2.0^\circ$. The intensities of individual peaks were obtained by applying a peak-decomposition program using the shape of the well-separated peak at 0.994 MeV as a reference. Among the clearly observed states listed in Table I, all states, except the three states at 0.803, 1.375, and 2.867 MeV showed a similar relative decrease of their strengths with increasing Θ. We judge that transitions to all these states are of $L = 0$ nature. Among the three $L \geqslant 1$ states, the 0.803 MeV state, identified as the lowest $J^\pi = 3^+$ state in Ref. [23], was the strongest. In addition, the angular distribution of this state is not fully understood. It showed a similar relative decrease in the angle cuts up to $1.0^\circ - 1.5^\circ$. A relatively large increase of 50% of the intensity was observed only in the $1.5^\circ - 2.0^\circ$ cut. The relative intensities of the other two $L \geqslant 1$ states increased by more than 50% already in the $0.5^\circ - 1.0^\circ$ cut in the comparison with the $0^\circ - 0.5^\circ$ cut.

It is known that the g.s. of ^{46}V is the IAS of ^{46}Ti [23]. Because the Fermi transition strength is concentrated in the IAS, it is very probable that the other $L = 0$ states are all GT states with the J^π values of 1^+.

III. DATA ANALYSIS

A. B(GT) evaluation from (^{3}He,t) data

It is known that in CE reactions at 0° and at intermediate incident energies above 100 MeV/nucleon the cross sections for GT transitions are approximately proportional to the B(GT) values [3,29]:

$$\frac{d\sigma_{GT}}{d\Omega}(0^\circ) \simeq K_{GT}\, N_{GT}\, |J_{\sigma\tau}(0)|^2 B(GT) \quad (1)$$

$$= \hat{\sigma}_{GT}(0^\circ) B(GT), \quad (2)$$

where $J_{\sigma\tau}(0)$ is the volume integral of the effective interaction $V_{\sigma\tau}$ at momentum transfer $q = 0$, K_{GT} is the kinematic factor, N_{GT} is a distortion factor, and $\hat{\sigma}_{GT}(0^\circ)$ is the unit cross section for the GT transition. For (^{3}He, t) reactions, this approximate proportionality was shown for the transitions with B(GT) values $\geqslant 0.04$ and with $L = 0$ nature from the studies of analogous GT transitions in $A = 27$; $T = 1/2$ mirror nuclei ^{27}Al and ^{27}Si [12]; and $A = 26$ nuclei ^{26}Mg, ^{26}Al, and ^{26}Si [13]. Here we use a unit system that gives a value of $B(GT) = 3$ for the β decay of the free neutron. However, deviations are predicted for *fp*-shell nuclei [30]; the proportionality constant may depend on the single particle orbit and may differ for $1f$ and $2p$ levels that differ in the number of radial nodes. The reason is that the (^{3}He, t) reaction is a surface reaction. Of course such effect mingles the reaction and the nuclear structure aspects and vastly complicates the analysis of the data. The effect, however, is expected to be small in the region where the $f_{7/2}$ shell is at the Fermi level, i.e., below $N = Z \leqslant 27$, where the nucleus ^{46}V is situated. It is, however, still important to be aware of this effect.

A similar proportionality given by Eq. (1) is expected for the Fermi transition with $\Delta L = 0$ nature, i.e., for the transition to the IAS [3]:

$$\frac{d\sigma_F}{d\Omega}(0^\circ) \simeq K_F\, N_F\, |J_\tau(0)|^2 B(F) \quad (3)$$

$$= \hat{\sigma}_F(0^\circ) B(F), \quad (4)$$

where $J_\tau(0)$ is the volume integral of the effective interaction V_τ at momentum transfer $q = 0$, K_F is the kinematic factor, N_F is a distortion factor, and $\hat{\sigma}_F(0^\circ)$ is the unit cross section for the transition to the IAS.

It is known that the product $K_{GT}N_{GT}$ in Eq. (1) gradually changes as a function of excitation energy [3]. To estimate this effect, a distorted-wave Born approximation (DWBA) calculation was performed by using the code DW81 [31] and assuming a pure $f_{7/2} \rightarrow f_{5/2}$ transition for the excited GT states. We used optical potential parameters determined for ^{58}Ni at an incident ^{3}He energy of 150 MeV/nucleon [32]. For the outgoing triton channel, the well depths were multiplied by

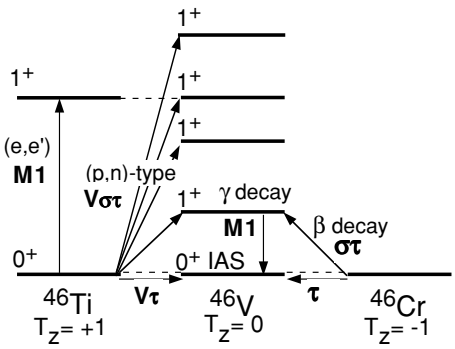

FIG. 2. Isospin analogous transitions in the $A = 46$, $T_z = \pm 1$ and 0 isobar system are schematically shown. The Coulomb displacement energies are removed so that the isospin symmetry of the system and that of transitions are put in evidence. Analog states with $T = 1$ are connected by broken lines. The type of the reaction or decay and the relevant interaction causing each transition are shown along the arrows indicating the transitions.

a factor of 0.85 without changing the geometrical parameters of the optical potential following the arguments given in Ref. [33]. For the effective projectile-target interaction of the composite ^{3}He particle, the form derived by Schaeffer [34] through a folding procedure was used. As the interaction strength $V_{\sigma\tau}$ and the range R, we used the values of -2.1 MeV and 1.415 fm, respectively [35]. The calculated 0° cross section decreases by about 4% as E_x increases up to 4.5 MeV. This result was used to correct the peak intensity of each state.

To derive B(GT) values from Eq. (1), a standard B(GT) value, preferably determined in a β-decay measurement, is needed. The β decay of ^{46}V g.s. to g.s. of ^{46}Ti is well studied [36]. Since the g.s. of ^{46}V having $J^\pi = 0^+$ is the IAS of ^{46}Ti, the transition is of pure Fermi character [23] and no information on the GT strength is available. Under the assumption that isospin T is a good quantum number, the GT transitions from the g.s. of $T_z = \pm 1$ nuclei ^{46}Ti and ^{46}Cr to the $T_z = 0$ nucleus ^{46}V are analogous, where T_z [$= (N - Z)/2$] is the z component of isospin T (see Fig. 2). Recently the β decay from ^{46}Cr to ^{46}V was measured using the ^{46}Cr beam produced by a projectile-fragment separator [37]. Assuming that the analogous GT transitions have the same B(GT) values, the B(GT) values from the β decay can in principle be used as "standard B(GT) values." However, a B(GT) value with relatively large ambiguity was derived only for the lowest lying GT state in this β-decay study. Recently a merged analysis that combines the excitation strengths of discrete states from the (^{3}He,t) measurement and the Q value and the half-life $T_{1/2}$ from the isospin analogous β decay was proposed to derive the absolute B(GT) values assuming the mirror symmetry of the $T_z = \pm 1 \rightarrow 0$ GT transitions [38]. The method was applied to the GT transitions in the $A = 50$ isobar nuclei ^{50}Cr, ^{50}Mn, and ^{50}Fe and absolute B(GT) values were derived. The application of this merged analysis to the $A = 46$ system, however, was unsuccessful. It was found that the large relative uncertainties of 23% in the $T_{1/2}$ value (260 ± 60 ms) of ^{46}Cr leads to a relative uncertainty of more than 50% in the B(GT) values.

To derive the B(GT) values for the $A = 46$ nuclei, we use here the transition strength to the IAS as a standard assuming the following: (1) all the Fermi transition strength concentrates in the IAS, and it consumes the complete sum-rule value of $B(\mathrm{F}) = N - Z$, and (2) the ratio of GT and Fermi unit cross sections denoted as R^2 [3] and defined by

$$R^2 = \frac{\hat{\sigma}_{\mathrm{GT}}(0^\circ)}{\hat{\sigma}_{\mathrm{F}}(0^\circ)} = \frac{\sigma_{\mathrm{GT}}(0^\circ)}{B(\mathrm{GT})} \Big/ \frac{\sigma_{\mathrm{F}}(0^\circ)}{B(\mathrm{F})} \tag{5}$$

is a constant for a given mass number A and is a smooth function of A. Recently, the A dependence of R^2 was systematically studied, and a smooth increase of R^2 was observed as a function of A. A value of 7.7(9) can be deduced for the $A = 46$ nuclei by quadratically interpolating the experimentally obtained R^2 values of 5.8(4), 6.6(2), 8.7(8), 8.7(6), and 8.8(4) for the $A = 18$, 26, 62, 64, and 68 nuclei [13,39], respectively.

An accurate Fermi cross-section (or intensity) of the transition to the IAS (the g.s. of ^{46}V) is needed to obtain the GT unit cross section (or the unit GT intensity) using the R^2 value. For doing this, one has to take into account that all IASs originating from different titanium isotopes are expected to have similar Q values because the latter quantities represent the Coulomb displacement energies (CDE) between the g.s. of the target nucleus, and the IAS under consideration. The CDE is mainly dependent on the proton number Z of the target nucleus, and not so much on the mass number A. A careful examination of the peak shape of the IAS in the ^{46}V spectrum showed that the bottom part was wider by several kiloelectron volts, and had an extended tail, suggesting that there are some contributions from other titanium isotopes.

To estimate the accurate Fermi intensity of the transition to the IAS originating purely from ^{46}Ti, contributions from the ^{47,48,49,50}Ti isotopes should be subtracted. It is noted that the Fermi transition strengths have $B(\mathrm{F}) = N - Z$. We assume the same unit Fermi cross section for all isotopes. The IASs originating from the even isotopes ^{48}Ti and ^{50}Ti contain only the Fermi transition strength. Using the known isotopic abundances of 10.6(1)% and 1.0(1)% of these isotopes in the used ^{46}Ti target and assuming the B(F) values of 4 and 6, it was estimated that the contributions of them in the observed IAS peak were 18.1(2)% and 2.6(3)%, respectively. However, the IASs originating from the odd isotopes ^{47}Ti and ^{49}Ti contain not only the Fermi strength but also the GT strength [40]. Because the ^{47}V spectrum has been obtained in the ^{47}Ti(^{3}He, t) measurement, the contribution from the ^{47}Ti isotope [abundance 1.6(1)% in the ^{46}Ti target] could be estimated experimentally. By comparing the ^{46}V and ^{47}V spectra, it was found that not only the IAS peak but also a few nearby GT states of ^{47}V were included in the tail part of the IAS peak in the ^{46}V spectrum. It was estimated that their contribution amounted to 3.9(7)% of the ^{46}V IAS peak. Because a (^{3}He, t) spectrum for a ^{49}Ti target was not available, a minimum contribution of 1.7(2)% from the ^{49}Ti isotope [abundance 0.8(1)%] could be estimated by assuming a pure Fermi transition and $B(\mathrm{F}) = 5$. As a result, it was estimated that the Fermi intensity originating from ^{46}Ti was 73.7% of the IAS peak in our ^{46}V spectrum with a probable uncertainty of 1.5%.

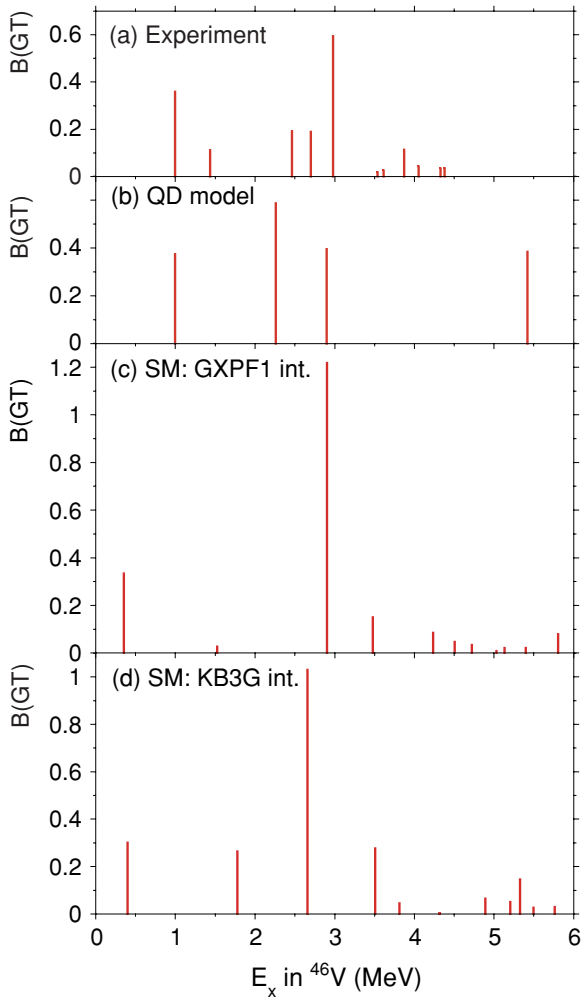

FIG. 3. (Color online) Comparison of experimental and theoretical B(GT) strength distributions. (a) Measured B(GT) distribution from the ^{46}Ti(^{3}He,t)^{46}V reaction. (b) B(GT) distribution from a QD-model calculation. (c) B(GT) distribution from a shell-model calculation using the GXPF1 interaction. (d) B(GT) strengths from a shell-model calculation using the KB3G interaction. Note the change of the ordinate range of the panels.

The unit GT intensity for the 0° spectrum was calculated by using the R^2 value and the unit Fermi intensity estimated above. The B(GT) values for other excited states were calculated from their peak intensities, after correcting for the excitation energy dependence using the DWBA calculation, assuming the proportionality of Eq. (2). The DWBA correction was about 4% at 4.5 MeV. It was found that the states at 1.433 and 2.699 MeV were overlapping with ^{48}V states. The contributions from these ^{48}V states were estimated from the ^{48}V spectrum and subtracted. The deduced B(GT) values are listed in column 5 of Table I and are shown in Fig. 3(a), where the uncertainties are mainly because of those of the R^2 value. Although the detailed analysis was performed only up to 4.5 MeV, we can exclude the existence of strong GT transitions to the energy range from 4.5 to 6 MeV, as is clear from Fig. 1.

IV. DISCUSSION

A. GT strengths

1. Comparison with the β-decay result

As discussed above, the transitions from the g.s. of ^{46}Cr to the GT states in ^{46}V are analogous with those observed in the ^{46}Ti(^{3}He,t)^{46}V reaction. The result of the ^{46}Cr β-decay measurement was reported recently [37]. Because of a relatively small yield of the proton-rich nucleus ^{46}Cr, the B(GT) value of 0.64 ± 0.20 with a rather large uncertainty was obtained only for the first GT state at 0.994 MeV. This B(GT) value is 75% larger than our value of 0.37 ± 0.04. In Ref. [37] the branching ratio to this state was deduced by measuring the number of the 0.994 MeV γ rays relative to the number of the incoming ^{46}Cr nuclei. Note that the proton separation energy S_p of ^{46}V is 5.356 MeV [41] and that we found additional 10 candidates of GT state even in the region below $E_x = 4.5$ MeV. Some feeding from higher excited states to this 0.994 MeV state is also known [25]. Therefore, we suspect that the B(GT) value given in Ref. [37] represents an upper limit. A further investigation of the ^{46}Cr β decay with a better accuracy, not only for the branching ratios, but also for the half-life, is certainly desirable.

2. Comparison with theoretical calculations

We compare the measured GT strength distribution with the predictions obtained from three different models, i.e., the quasideuteron (QD) model with a deformed core (rotor-plus-quasideuteron model) [42] and the shell model (SM) with the GXFP1 [6] and the KB3G [7] effective interactions. The calculated excitation energies of 1^+ states in ^{46}V and the B(GT) values multiplied by the usual quenching factor of $(0.74)^2$ [43] are shown in Table II. They are compared with the experimental results in Fig. 3.

The QD model with a deformed core can give a simplified pictorial view of the structure for low-lying states in a deformed odd-odd nucleus [13,42]. The low-lying states in ^{46}V are described by an angular-momentum-coupled proton-neutron pair or a quasideuteron (a generalized deuteron) made of the valence odd proton and neutron occupying Nilsson orbitals coupled to the rotating ^{44}Ti core. A recent γ-ray spectroscopy measurement for the low-lying region of ^{46}V [25,44] was described by this approach. The measured $B(E2)$ values suggested a substantial quadrupole deformation of $\beta \approx 0.28$.

In the QD model, the $T = 1$, $J^\pi = 0^+$ g.s. and the first $T = 0$, 1^+ state of ^{46}V are described by assuming that both odd nucleons mainly occupy the identical Nilsson orbital $[321]3/2^-$ closest to the Fermi surface. This single-particle orbital, originating from the $f_{7/2}$ shell, is characterized by $\Omega^\pi = 3/2^-$, where Ω is the z component (the component along the symmetry axis of the rotor) of the total angular momentum of the single particle. These odd nucleons can couple to $K = 0$ and also to $K = 3$, where $K(= 2\Omega)$ is the z component of the total angular momentum of the quasideuteron. Therefore, $K = 0$ is assigned to the $T = 1$, 0^+ g.s. (IAS) and to the lowest $T = 0$, 1^+_1 state [13]. The experimentally available data on the

TABLE II. Excitation energies of $J^\pi = 1^+$ states in ^{46}V and GT transition strengths from the g.s. of ^{46}Ti calculated within the QD model and shell model with KB3G and GXFP1 effective interactions. Results up to about $E_x = 6$ MeV are shown. The B(GT) values include a quenching factor of $(0.74)^2$.

QD		KB3G		GXPF1	
E_x	B(GT)	E_x	B(GT)	E_x	B(GT)
0.994	0.375	0.399	0.302	0.351	0.334
2.258	0.587	1.775	0.264	1.521	0.028
2.895	0.395	2.655	1.030	2.899	1.218
5.420	0.384	3.507	0.278	3.478	0.151
		3.809[a]	0.046	4.234[a]	0.086
		4.312	0.004	4.505	0.047
		4.890	0.066	4.721	0.035
		5.201	0.051	5.027	0.009
		5.325[a]	0.147	5.131	0.022
		5.495	0.027	5.396	0.021
		5.597	0.002	5.805[a]	0.080
		5.763	0.030	5.960	0.001

[a]Isospin $T = 1$ is assigned.

$M1$ transition between these states in ^{46}V clearly supports the above assignment [45]. The experimental B(GT) value of 0.365 for the first 1^+ state is well reproduced by the QD model as well as by the shell models.

The second and the third 1^+, $T = 0$ states are described by the excitation of one nucleon from the $\Omega^\pi = 3/2^-$ to the higher $\Omega^\pi = 5/2^-$ orbital and from the lower $\Omega^\pi = 1/2^-$ (by breaking one pair) to the $\Omega^\pi = 3/2^-$ orbital, respectively. Because of the $\Delta\Omega = 1$ nature of these excitations, $K = 1$ is assigned to these states. It is noted that the structure of three orbitals involved in the formation of the lowest three 1^+ states is dominated by the $f_{7/2}$ orbital. This causes relatively large B(GT) values, because a large $\langle f_{7/2}\|\sigma\tau\|f_{7/2}\rangle$ GT matrix element (m.e.) constructively interferes with the smaller spin-flip $\langle f_{7/2}\|\sigma\tau\|f_{5/2}\rangle$ m.e., thus enhancing the GT strength (for details, see Ref. [46]).

As we see from Fig. 3 and Table II, the observed three GT states in the $E_x = 2.5-3.0$ MeV region seem to correspond to the second 1^+ state at 2.258 MeV in the QD model and the strong 2.655- and 2.899-MeV states in the SM calculations using the KB3G and the GXPF1 interactions, respectively. The observed splitting of these single states into three states may suggest the contribution of the ^{40}Ca core excitation, as discussed below. The fragmented GT states observed in the $E_x = 3.5$–4.5 MeV region seem to correspond to the third 1^+ state of the QD model. The observed fragmentation is reproduced to some extent by the KB3 interaction and better reproduced by the GXPF1 interaction. The splitting of the GT strength in the SM calculations shows that there are more complicated couplings of the proton-neutron pair to the even-even cluster of four nucleons in the full *fp* shell that are not taken into account in the QD model.

A few $T = 1$ states are predicted in the SM calculations between $E_x = 4-6$ MeV (see Table II). The isospin of the observed GT states are discussed in Sec. IVB. The summed GT strengths up to 4.5 MeV are 1.36 in the QD model, 1.93 and 1.86 in the SM calculation using the KB3G and the GXPF1 interactions, respectively. They are all consistent within the respective uncertainties of about 20% with the experimentally observed value of 1.77.

We mentioned that two extra 1^+ states observed at energies below $E_x = 3.0$ MeV are not reproduced in any of the calculations. There are even more experimental 1^+ states above 3.5 MeV that are not reproduced in the shell model and the QD model. Because the SM calculations with different effective interactions in the full *fp* space give the same number of states below 3 MeV, one may conclude that these extra states are because of the ^{40}Ca core breaking. The structure of these extra states is expected to be dominated by configurations that involve the $d_{3/2}$ orbital. Because the $d_{3/2}$ orbital and its *LS* partner, the $d_{5/2}$ orbital, are almost completely filled, the expected GT strength is small. In addition, destructive interference is expected between the spin-nonflip GT m.e. $\langle d_{3/2}\|\sigma\tau\|d_{3/2}\rangle$ and the spin-flip m.e. $\langle d_{5/2}\|\sigma\tau\|d_{3/2}\rangle$, which can further suppress the GT strength [46]. Therefore, it is expected that the contribution of the core breaking is small to the GT strength itself, but the effect of it mainly appears as fragmentation of the GT states.

B. Isospin values and orbital/isoscalar contributions

Because of the isovector nature, the $(^3\mathrm{He}, t)$ reaction starting from the $T_0 = 1$ g.s. of ^{46}Ti excites $J^\pi = 1^+$ states with $T = 0$, 1, and 2 in ^{46}V. Because of the symmetry energy, the $T = 0$ GT states are found at low, the $T = 1$ states at intermediate, and the $T = 2$ states at high excitation energies [47]. Therefore, it is expected that most of the GT states observed here have $T = 0$, but the $T = 1$ states can also be in this region as predicted by the shell-model calculations shown in Table II. On the other hand, the 1^+ states in ^{46}Ti, which are usually called $M1$ states, can have $T = 1$ or 2. They are the isobaric analog states of the $T = 1$ or 2 GT states, respectively, assuming isospin symmetry structure for ^{46}Ti ($T_z = 1$) and ^{46}V ($T_z = 0$) (see Fig. 2). The $T = 1$ nature of the GT states in ^{46}V, therefore, can be studied by examining the existence of the analog $M1$ states in ^{46}Ti. For the identification of isospin T of the observed GT states, comparisons with inelastic reactions, such as ^{46}Ti(p, p'), (γ, γ'), or (e, e'), are needed [14].

Since the g.s. of ^{46}V is the IAS of the $T = 1$, $J^\pi = 0^+$ g.s. of ^{46}Ti, it is expected that $T = 1$ GT states in ^{46}V have almost the same excitation energies as the corresponding $M1$ states in ^{46}Ti. The excited states in ^{46}Ti with J^π values of 1^+ [23] are listed in Table III. In addition, states with $J^\pi = 0^+$ assignment are also listed to examine the possible fragmentation of the IAS. Among the four 1^+ or tentative 1^+ states in ^{46}Ti, no indication of corresponding state in ^{46}V was observed for the 3.731- and 3.906-MeV states. However, for the 3.872- and 4.316-MeV states, corresponding $L = 0$ states, probably with $J^\pi = 1^+$, are observed at 3.870 and 4.325 MeV in ^{46}V. Thus we can tentatively give $T = 1$, $J^\pi = 1^+$ assignment to them.

The comparison of the strengths of the analogous GT and $M1$ transitions gives us additional information on the structure of states. On the basis of the ^{46}Ti(γ, γ') measurement

TABLE III. Compilation of experimentally identified $J^\pi = 0^+$ and 1^+ states in ^{46}Ti and the corresponding states observed in the ^{46}Ti(^{3}He, t)^{46}V reaction for excitation energies below 4.5 MeV.

States in ^{46}Ti[a]						States in ^{46}V[b]			
		(γ, γ')[c]		(e, e')[d]		(^{3}He, t)			
E_x (MeV)	J^π	$B(M1)\uparrow$	$B^R(M1)$	$B(M1)\uparrow$	$B^R(M1)$	E_x (MeV)	B(GT)	$R_{\rm ISO}$[e]	T
0.0	0^+ [f]					0.0			1
2.611	0^+								
3.572	0^+								
3.731	1^+			0.27(6)	0.10(3)				
3.872	1^+			0.19(6)	0.07(3)	3.870	0.117(14)	0.5	1
3.906	$(1, 2^+)$								
4.316	1^+	0.55(8)[g]	0.21(3)	1.04(10)[g]	0.39(4)	4.325	0.034(5)	5–10	1

[a]From Ref. [23].
[b]Present work.
[c]From Ref. [48].
[d]From Ref. [49].
[e]$R_{\rm MEC} = 1.25$ is assumed.
[f]The IAS.
[g]$B(M1)\uparrow$ values from the (γ, γ') and (e, e') experiments are different by a factor of 2.

[48], 100% decay to the g.s. and a decay width of $\Gamma_0 = 0.172(26)$ eV were deduced for the 4.316 MeV state in ^{46}Ti. A $B(M1)\uparrow$ value of $0.55(8)\mu_N^2$ is calculated from these values for the $M1$ transition from the g.s. to this state (see e.g., Ref. [12]). In addition, a ^{46}Ti(e, e') measurement [49] gives $B(M1)\uparrow$ values for the transitions to the 3.731-, 3.872-, and 4.316-MeV states. They are listed in Table III.

To these electromagnetic $M1$ transitions, not only the IV spin $(\sigma\tau)$ term but also the isoscalar (IS) term and the isovector (IV) orbital $(\ell\tau)$ term of the $M1$ operator can contribute [50, 51]. The IS term is usually small [51] and in a spherical nucleus the contribution of the IV spin term is expected to be the largest [47]. The contribution of the orbital term, however, can be large if a nucleus is deformed, as was found for the $A = 23$ [52] and $A = 25$ [53] systems. As mentioned, for the $A = 46$ system a substantial quadrupole deformation of $\beta \approx 0.28$ was suggested by the analysis of the γ transitions between the low-lying low-spin states [44]. Therefore, it is interesting to compare the strengths of analogous GT and $M1$ transitions.

To compare the B(GT) and $B(M1)$ values, we take note of the fact that the IV spin term is common in both transitions. If there is only this IV spin contribution in an $M1$ transition, the $B(M1)\uparrow$ value of this $M1$ transition is proportional to the B(GT) value of the analogous GT transition. The relationship is given by [14]

$$B(M1)\uparrow = \frac{3}{8\pi}\,(\mu_p - \mu_n)^2\,\frac{C_{M1}^2}{C_{\rm GT}^2}\,R_{\rm MEC}\,B({\rm GT}), \qquad (6)$$

where C_{M1} is the isospin Clebsch-Gordan (CG) coefficient $(T_i T_{zi} 10|T_f T_{zf})$ with $T_{zf} = T_{zi}$ and $C_{\rm GT}$ is $(T_i T_{zi} 1 \pm 1|T_f T_{zf})$ with $T_{zf} = T_{zi} \pm 1$. The so-called meson exchange currents (MEC) affect $M1$ and GT transitions differently [54]. This is expressed by the parameter $R_{\rm MEC}$. An average value of 1.25 was obtained for *sd*-shell nuclei [51] by comparing experimental $B(M1)$ and B(GT) values with those from shell-model calculations. We tentatively use this value, although there is a suggestion that $R_{\rm MEC}$ may be smaller for *fp*-shell nuclei [55]. The numerical factor is $2.643\mu_N^2$ if the magnetic moments of free nucleons are used. The ratio of the squared CG coefficients is unity for transitions from the g.s. of ^{46}Ti to excited $M1$ and GT states with $T = 1$.

From Eq. (6), it is noticed that a $M1$ transition strength can be directly compared with the B(GT) value if the "renormalized $B(M1)\uparrow$" value

$$B^R(M1) = \frac{1}{2.643\mu_N^2}\,B(M1)\uparrow \qquad (7)$$

is defined [12,13,56], where the ratio of the squared CG coefficients is taken to be unity. The $B^R(M1)$ values deduced from the (γ, γ') and (e, e') measurements are listed in columns 4 and 6 of Table III. If we further calculate the ratio

$$R_{\rm ISO} = B^R(M1)/[R_{\rm MEC}\ B({\rm GT})] \qquad (8)$$

for the analogous $M1$ and GT transitions [12,56], then the ratio $R_{\rm ISO}$ can be larger or smaller than unity depending on the constructive or the destructive interference of the orbital (and may be isoscalar) contribution.

For the two pairs of transitions to $M1$ and GT states with good corresponding E_x values, $R_{\rm ISO}$ values were derived and given in column 9 of Table III. For the pair of states at 3.872 and 3.870 MeV in ^{46}Ti and ^{46}V, respectively, an $R_{\rm ISO}$ value of 0.5 is obtained. This value smaller than unity suggests a destructive interference between the IV-spin and IV-orbital terms in the $M1$ transition under the assumption that the IS term is small. However, for the pair of states at 4.316 and 4.325 MeV, we obtain a very large $R_{\rm ISO}$ value of 5−10. Therefore, a constructive interference of the IV-spin and IV-orbital terms is suggested in this $M1$ transition. It should be noted that the obtained $R_{\rm ISO}$ value of 5−10 is one of the largest values ever observed, even compared with the $R_{\rm ISO}$ values observed for the $M1$ transitions in well-deformed *sd*-shell nuclei, like ^{23}Na [52] and ^{25}Mg [53].

In the region around $E_x = 4$ MeV in ^{46}V, the SM calculations with the KB3G and GXPF1 interactions predict $T = 1, 1^+$ states at 3.809 MeV and at 4.234 MeV, respectively (see Table II). For the corresponding analogous $M1$ transition in ^{46}Ti, $B(M1)\uparrow$ [$B^R(M1)$] values of 0.772[0.292] and 1.038[0.393], respectively, are calculated by these interactions. Constructive interference is predicted for the IV-spin and IV-orbital terms and $R_{\rm ISO}$ values of about five are estimated. It is suggested that these calculated $T = 1$ states correspond to the 4.325-MeV state in ^{46}V (4.316-MeV state in ^{46}Ti) having a similar $R_{\rm ISO}$ value. However, no state corresponding to the 3.870-MeV state in ^{46}V (3.872-MeV state in ^{46}Ti) is predicted in these SM calculations. It is suggested that the main contribution to this 3.870-MeV state comes from the configurations of the *sd* shell that are not included in the present SM calculations.

The $M1$ γ transition from an excited 1^+ state to the g.s. of ^{46}V is analogous with the GT transition from the g.s. of ^{46}Ti to this excited 1^+ state in ^{46}V, as seen from Fig. 2. A lower limit of $B(M1)\uparrow \geqslant 2.31\mu_N^2$ has been experimentally obtained for the $M1$ transition from the g.s. of ^{46}V ($T = 1$) to the 0.994-MeV, 1^+ state ($T = 0$) [45]. Because this transition has the $\Delta T = 1$ nature, no contribution from the IS term is expected. Therefore, the effect of the interference of the IV-spin and IV-orbital terms in this $M1$ transition can be directly estimated by calculating the ratio $R_{\rm ISO}$. For $M1$ transitions from a $T_i = 1$ state to $T_f = 0$ states in ^{46}V, we obtain $C^2_{M1} = (1010|00)^2 = 1/3$. Similarly, for GT transitions from a $T_i = 1$ state in ^{46}Ti to $T_f = 0$ states in ^{46}V, $C^2_{\rm GT} = (111 - 1|00)^2 = 1/3$ is calculated. Therefore, the ratio of the squared CG coefficients in Eq. (6) is unity, and the $B^R(M1)$ value is obtained by using Eq. (7). Again by assuming $R_{\rm MEC} = 1.25$, we obtain $R_{\rm ISO} \geqslant 2.5$, showing a constructive interference of the IV-spin and IV-orbital terms.

As it has been pointed out, in the QD model the $J^\pi = 0^+, T = 1$ g.s. and the first $T = 0, 1^+$ state of ^{46}V can be described by assuming that both the odd proton and neutron mainly occupy the identical Nilsson orbital $[321]3/2^-$ that originates from the $f_{7/2}$ shell. It is known that the spin and orbital contributions are constructive if the configuration involved in the transition is the so-called high j ($= \ell + 1/2$) type, like $f_{7/2}$ [13,42,57]. Similar constructive and destructive interferences of $\sigma\tau$ and $\ell\tau$ terms in relation to high-j and low-j configurations, respectively, have been observed and discussed for the $M1$ transitions in deformed *sd*-shell nuclei [52,53,56].

V. SUMMARY

GT transitions were studied in the ^{46}Ti(^{3}He, t)^{46}V reaction at the intermediate beam energy of 140 MeV/nucleon. Owing to the high energy resolution of 33 keV, states up to $E_x = 4.5$ MeV in ^{46}V were clearly separated. The relative energy resolution of $\Delta E/E = 10^{-4}$ achieved here is based on the successful implementation of dispersion matching between the spectrometer and the beam line.

The high energy resolution of the spectrum allowed to determine the level energies and intensities of excited states accurately even for weakly populated states. In the (^{3}He, t) reaction at 140 MeV/nucleon, a good proportionality between the B(GT) value and the cross section at 0° is expected and the study of B(GT) values can be extended to high excitations. For the $A = 46$ system, there is no accurate standard B(GT) value available from a β-decay measurement. Therefore, the B(GT) values were derived by the interpolation of the mass A systematics of the R^2 value defined by the ratio of the unit GT cross-section $\hat{\sigma}_{\rm GT}$ and the unit Fermi cross-section $\hat{\sigma}_F$.

The derived GT strength distribution was compared with theoretical predictions. At present the GT strength distributions for some of the *fp*-shell nuclei that are important in presupernova models are hard to measure in experiments directly. Therefore, it is important to examine the predictive power of theoretical calculations. The quasideuteron model and the shell-model calculations using the KB3G and the GXPF1 interactions, including the usual quenching factor of $(0.74)^2$, could reproduce the experimental strength up to 4.5 MeV excitation. However, the fragmentation of the GT strength, especially in the low-lying region for excitation energies up to 3 MeV, was not so well reproduced, suggesting an excitation of the *sd*-shell core that was assumed to be inert in the theoretical models.

The 1^+ GT states of ^{46}V in the energy region studied here can have isospin values $T = 0$ or 1, whereas the 1^+ $M1$ states in ^{46}Ti excited in the inelastic reactions have $T = 1$. To identify the isospin T of observed GT states, corresponding $M1$ states were looked for in the results of (γ, γ') and (e, e') measurements. For the two states at 3.870 and 4.325 MeV, candidates of analog $M1$ states were found, suggesting that they are the $T = 1$ states. By comparing the strengths of analogous $M1$ and GT transitions, a constructive contribution of the IV-orbital and IV-spin terms was found in the $M1$ transition from the 4.316-MeV state to the g.s. of ^{46}Ti. A similar constructive contribution was suggested for the $M1$ transition from the 0.994-MeV state to the g.s. of ^{46}V.

ACKNOWLEDGMENTS

This work was in part supported by Monbukagakusho (MEXT), Japan, under grant no. 15540274 and Specially Promoted Research grant no. 13002001, and DFG, Germany under contracts Br 799/12-1, Jo 391/2-1, and Pi 393/1-2. The (^{3}He, t) experiments were performed at RCNP, Osaka University, under the experimental programs E197 and E237. The authors are grateful to the accelerator group of RCNP, especially to Professor Saito and Dr. Ninomiya, for providing a high-quality ^{3}He beam. Y.F. thanks Professor I. Hamamoto (LTH, Lund, Sweden) for valuable discussions. The Gent group acknowledges support from the FWO-Flanders. G.P.A.B. acknowledges support from JSPS. T.A., L.P. and A.N. acknowledge support from the 21st Century COE program "Toward a new basic science" of Graduate School of Science, Osaka University. The shell-model calculation was performed as a part of the RIKEN-CNS joint research project on large-scale nuclear-structure calculations. The Köln group and the Gent group thank the people at RCNP for their hospitality during their stay for the experiment.

[1] K. Langanke and G. Martínez-Pinedo, Rev. Mod. Phys. **75**, 819 (2003).
[2] G. M. Fuller, W. A. Fowler, and M. J. Newman, Astrophys. J. Suppl. Ser. **42**, 447 (1980); **48**, 279 (1982); Astrophys. J. **252**, 715 (1982); **293**, 1 (1985).
[3] T. N. Taddeucci, C. A. Goulding, T. A. Carey, R. C. Byrd, C. D. Goodman, C. Gaarde, J. Larsen, D. Horen, J. Rapaport, and E. Sugarbaker, Nucl. Phys. **A469**, 125 (1987), and references therein.
[4] J. Rapaport and E. Sugarbaker, Annu. Rev. Nucl. Part. Sci. **44**, 109 (1994).
[5] E. Caurier, G. Martínez-Pinedo, F. Nowacki, A. Poves, J. Retamosa, and A. P. Zuker, Phys. Rev. C **59**, 2033 (1999).
[6] M. Honma, T. Otsuka, B. A. Brown, and T. Mizusaki, Phys. Rev. C **69**, 034335 (2004).
[7] A. Poves, J. Sánchez-Solano, E. Caurier, and F. Nowacki, Nucl. Phys. **A694**, 157 (2001).
[8] E. Caurier, K. Langanke, G. Martínez-Pinedo, and F. Nowacki, Nucl. Phys. **A653**, 439 (1999).
[9] K. Langanke and G. Martínez-Pinedo, Nucl. Phys. **A673**, 481 (2000).
[10] Y. Fujita, K. Hatanaka, G. P. A. Berg, K. Hosono, N. Matsuoka, S. Morinobu, T. Noro, M. Sato, K. Tamura, and H. Ueno, Nucl. Instrum. Methods B **126**, 274 (1997); and references therein.
[11] Y. Fujita, T. Adachi, H. Akimune, A. D. Bacher, G. P. A. Berg, T. Black, I. Daito, C. C. Foster, H. Fujimura, H. Fujita, M. Fujiwara, K. Hara, K. Harada, M. N. Harakeh, K. Hatanaka, T. Inomata, J. Jänecke, J. Kamiya, Y. Kanzaki, K. Katori, T. Kawabata, W. Lozowski, K. Nagayama, T. Noro, D. A. Roberts, H. Sakaguchi, Y. Shimbara, T. Shinada, E. J. Stephenson, A. Tamii, K. Tamura, M. Tanaka, H. Ueno, T. Wakasa, T. Yamanaka, M. Yoshifuku, and M. Yosoi, Nucl. Phys. **A687**, 311c (2001).
[12] Y. Fujita, H. Akimune, I. Daito, H. Fujimura, M. Fujiwara, M. N. Harakeh, T. Inomata, J. Jänecke, K. Katori, A. Tamii, M. Tanaka, H. Ueno, and M. Yosoi, Phys. Rev. C **59**, 90 (1999).
[13] Y. Fujita, Y. Shimbara, A. F. Lisetskiy, T. Adachi, G. P. A. Berg, P. von Brentano, H. Fujimura, H. Fujita, K. Hatanaka, J. Kamiya, T. Kawabata, H. Nakada, K. Nakanishi, Y. Shimizu, M. Uchida, and M. Yosoi, Phys. Rev. C **67**, 064312 (2003).
[14] Y. Fujita, H. Fujita, T. Adachi, G. P. A. Berg, E. Caurier, H. Fujimura, K. Hara, K. Hatanaka, Z. Janas, J. Kamiya, T. Kawabata, K. Langanke, G. Martínez-Pinedo, T. Noro, E. Roeckl, Y. Shimbara, T. Shinada, S. Y. van der Werf, M. Yoshifuku, M. Yosoi, and R. G. T. Zegers, Eur. Phys. J. A **13**, 411 (2002); H. Fujita, Ph.D. thesis, Osaka University, 2002.
[15] A. Jokinen, M. Oinonen, J. Äystö, P. Baumann, P. Dendooven, F. Didierjean, V. Fedoseyev, A. Huck, Y. Jading, A. Knipper, M. Koizumi, U. Köster, J. Lettry, P. O. Lips, W. Liu, V. Mishin, M. Ramdhane, H. Ravn, E. Roeckl, V. Sebastian, G. Walter, and ISOLDE Collaboration, Eur. Phys. J. A **3**, 271 (1998).
[16] W. G. Love and M. A. Franey, Phys. Rev. C **24**, 1073 (1981).
[17] T. Wakasa, K. Hatanaka, Y. Fujita, G. P. A. Berg, H. Fujimura, H. Fujita, M. Itoh, J. Kamiya, T. Kawabata, K. Nagayama, T. Noro, H. Sakaguchi, Y. Shimbara, H. Takeda, K. Tamura, H. Ueno, M. Uchida, M. Uraki, and M. Yosoi, Nucl. Instrum. Methods A **482**, 79 (2002).
[18] M. Fujiwara, H. Akimune, I. Daito, H. Fujimura, Y. Fujita, K. Hatanaka, H. Ikegami, I. Katayama, K. Nagayama, N. Matsuoka, S. Morinobu, T. Noro, M. Yoshimura, H. Sakaguchi, Y. Sakemi, A. Tamii, and M. Yosoi, Nucl. Instrum. Methods A **422**, 484 (1999).
[19] See http://www.rcnp.osaka-u.ac.jp.
[20] T. Noro *et al*., RCNP (Osaka Univ.), Annual Report, 1991, p. 177.
[21] H. Fujita, Y. Fujita, G. P. A. Berg, A. D. Bacher, C. C. Foster, K. Hara, K. Hatanaka, T. Kawabata, T. Noro, H. Sakaguchi, Y. Shimbara, T. Shinada, E. J. Stephenson, H. Ueno, and M. Yosoi, Nucl. Instrum. Methods A **484**, 17 (2002).
[22] Y. Fujita, H. Fujita, G. P. A. Berg, K. Harada, K. Hatanaka, T. Kawabata, T. Noro, H. Sakaguchi, T. Shinada, Y. Shimbara, T. Taki, H. Ueno, and M. Yosoi, J. Mass Spectrom. Soc. Jpn. **48(5)**, 306 (2000).
[23] S.-C. Wu, Nucl. Data Sheets **91**, 1 (2000).
[24] H. Fujita, G. P. A. Berg, Y. Fujita, K. Hatanaka, T. Noro, E. J. Stephenson, C. C. Foster, H. Sakaguchi, M. Itoh, T. Taki, K. Tamura, and H. Ueno, Nucl. Instrum. Methods A **469**, 55 (2001).
[25] C. Frießner, N. Pietralla, A. Schmidt, I. Schneider, Y. Utsuno, T. Otsuka, and P. von Brentano, Phys. Rev. C **60**, 011304(R) (1999).
[26] P. M. Endt, Nucl. Phys. **A521**, 1 (1990); **A633**, 1 (1998), and references therein.
[27] D. R. Tilley, H. R. Weller, and C. M. Cheves, Nucl. Phys. **A564**, 1 (1993).
[28] Y. Shimbara, Y. Fujita, M. Hamaguchi, E. Mochizuki, T. Adachi, G. P. A. Berg, H. Fujimura, H. Fujita, K. Fujita, K. Hara, K. Hatanaka, J. Kamiya, K. Kawase, T. Kawabata, Y. Kitamura, K. Nakanishi, N. Sakamoto, Y. Sakemi, Y. Shimizu, Y. Tameshige, M. Uchida, T. Wakasa, K. Yamasaki, M. Yoshifuku, and M. Yoshi, Nucl. Instrum. Methods A **522**, 205 (2004).
[29] W. G. Love, K. Nakayama, and M. A. Franey, Phys. Rev. Lett. **59**, 1401 (1987).
[30] K. Muto, private communications.
[31] DW81, a DWBA computer code by J. R. Comfort (1981) and updated version (1986), an extended version of DWBA70 by R. Schaeffer and J. Raynal (1970).
[32] T. Yamagata, H. Utsunomiya, M. Tanaka, S. Nakayama, N. Koori, A. Tamii, Y. Fujita, K. Katori, M. Inoue, M. Fujiwara, and H. Ogata, Nucl. Phys. **A589**, 425 (1995).
[33] S. Y. van der Werf, S. Brandenburg, P. Grasdijk, W. A. Sterrenburg, M. N. Harakeh, M. B. Greenfield, B. A. Brown, and M. Fujiwara, Nucl. Phys. **A496**, 305 (1989).
[34] R. Schaeffer, Nucl. Phys. **A164**, 145 (1971).
[35] R. G. T. Zegers, H. Abend, H. Akimune, A. M. van den Berg, H. Fujimura, H. Fujita, Y. Fujita, M. Fujiwara, S. Galés, K. Hara, M. N. Harakeh, T. Ishikawa, T. Kawabata, K. Kawase, T. Mibe, K. Nakanishi, S. Nakayama, H. Toyokawa, M. Uchida, T. Yamagata, K. Yamasaki, and M. Yosoi, Phys. Rev. Lett. **90**, 202501 (2003); S. Y. van der Werf and R. G. T. Zegers (private communication).
[36] G. Savard, F. Buchinger, J. A. Clark, J. E. Crawford, S. Gulick, J. C. Hardy, A. A. Hecht, J. K. P. Lee, A. F. Levand, N. D. Scielzo, H. Sharma, K. S. Sharma, I. Tanihata, A. C. C. Villari, and Y. Wang, Phys. Rev. Lett. **95**, 102501 (2005).
[37] T. K. Onishi, A. Gelberg, H. Sakurai, K. Yoneda, N. Aoi, N. Imai, H. Baba, P. von Brentano, N. Fukuda, Y. Ichikawa, M. Ishihara, H. Iwasaki, D. Kameda, T. Kishida, A. F. Lisetskiy, H. J. Ong, M. Osada, T. Otsuka, M. K. Suzuki, K. Ue,

Y. Utsuno, and H. Watanabe, Phys. Rev. C **72**, 024308 (2005).
[38] Y. Fujita, T. Adachi, P. von Brentano, G. P. A. Berg, C. Fransen, D. De Frenne, H. Fujita, K. Fujita, K. Hatanaka, E. Jacobs, K. Nakanishi, A. Negret, N. Pietralla, L. Popescu, B. Rubio, Y. Sakemi, Y. Shimbara, Y. Shimizu, Y. Tameshige, A. Tamii, and M. Yosoi, Phys. Rev. Lett. **95**, 212501 (2005).
[39] Y. Fujita *et al*., Experimental Proposal E237, RCNP, Osaka University; http://www.rcnp.osaka-u.ac.jp.
[40] Y. Fujita, Y. Shimbara, T. Adachi, G. P. A. Berg, B. A. Brown, H. Fujita, K. Hatanaka, J. Kamiya, K. Nakanishi, Y. Sakemi, S. Sasaki, Y. Shimizu, Y. Tameshige, M. Uchida, T. Wakasa, and M. Yosoi, Phys. Rev. C **70**, 054311 (2004).
[41] G. Audi, A. H. Wapstra, and C. Thibault, Nucl. Phys. **A729**, 337 (2003).
[42] A. F. Lisetskiy, A. Gelberg, R. V. Jolos, N. Pietralla, and P. von Brentano, Phys. Lett. **B512**, 290 (2001).
[43] G. Martínez-Pinedo, A. Poves, E. Caurier, and A. P. Zuker, Phys. Rev. C **53**, R2602 (1996).
[44] O. Möller, K. Jessen, A. Dewald, A. F. Lisetskiy, P. von Brentano, A. Fitzler, J. Jolie, A. Linnemann, B. Saha, and K. O. Zell, Phys. Rev. C **67**, 011301(R) (2003).
[45] P. von Brentano, A. F. Lisetskiy, C. Friessner, N. Pietralla, A. Schmidt, I. Schneider, R. V. Jolos, T. Otsuka, T. Sebe, and Y. Utsuno, Prog. Part. Nucl. Phys. **46**, 197 (2001).
[46] A. F. Lisetskiy, A. Gelberg, and P. von Brentano, Eur. Phys. J. A **26**, 51 (2005).
[47] A. Bohr and B. R. Mottelson, *Nuclear Structure* (Benjamin, New York, 1975), Vol. 2, Chap. 6.
[48] V. K. Rasmussen, Phys. Rev. C **13**, 631 (1976).
[49] T. Guhr, H. Diesener, A. Richter, C. W. de Jager, H. de Vies, and P. K. A. de Witt Huberts, Z. Phys. A **336**, 159 (1990).
[50] H. Morinaga and T. Yamazaki, In *Beam Gamma-Ray Spectroscopy* (North-Holland, Amsterdam, 1976), and references therein.
[51] Y. Fujita, B. A. Brown, H. Ejiri, K. Katori, S. Mizutori, and H. Ueno, Phys. Rev. C **62**, 044314 (2000).
[52] Y. Fujita, Y. Shimbara, I. Hamamoto, T. Adachi, G. P. A. Berg, H. Fujimura, H. Fujita, J. Görres, K. Hara, K. Hatanaka, J. Kamiya, T. Kawabata, Y. Kitamura, Y. Shimizu, M. Uchida, H. P. Yoshida, M. Yoshifuku, and M. Yosoi, Phys. Rev. C **66**, 044313 (2002).
[53] Y. Shimbara, Y. Fujita, T. Adachi, G. P. A. Berg, H. Fujita, K. Fujita, I. Hamamoto, K. Hatanaka, J. Kamiya, K. Nakanishi, Y. Sakemi, Y. Shimizu, M. Uchida, T. Wakasa, and M. Yosoi, Eur. Phys. J. A **19**, 25 (2004).
[54] I. S. Towner, Phys. Rep. **155**, 263 (1987).
[55] P. von Neumann-Cosel, A. Poves, J. Retamosa, and A. Richter, Phys. Lett. **B443**, 1 (1998).
[56] Y. Fujita, I. Hamamoto, H. Fujita, Y. Shimbara, T. Adachi, G. P. A. Berg, K. Fujita, K. Hatanaka, J. Kamiya, K. Nakanishi, Y. Sakemi, Y. Shimizu, M. Uchida, T. Wakasa, and M. Yosoi, Phys. Rev. Lett. **92**, 062502 (2004).
[57] I. Hamamoto and W. Nazarewicz, Phys. Lett. **B297**, 25 (1992).